Journal of the American College of Cardiology
© 2004 by the American College of Cardiology Foundation
Published by Elsevier Inc.

Vol. 43, No. 8, 2004
ISSN 0735-1097/04/$30.00
doi:10.1016/j.jacc.2003.09.065

Differential Diagnosis of Cardiac Masses Using Contrast Echocardiographic Perfusion Imaging

James N. Kirkpatrick, MD, Tiffany Wong, MD, James E. Bednarz, BS, RDCS, Kirk T. Spencer, MD, FACC, Lissa Sugeng, MD, R. Parker Ward, MD, FACC, Jeanne M. DeCara, MD, FACC, Lynn Weinert, BS, Thomas Krausz, MD, FRCPATH, Roberto M. Lang, MD, FACC

Chicago, Illinois

OBJECTIVES We investigated the usefulness of echocardiographic contrast perfusion imaging in differentiating cardiac masses.

BACKGROUND Two-dimensional echocardiography is the primary diagnostic modality for cardiac masses. However, differentiation between the different types of cardiac masses may be difficult at times. We hypothesized that echocardiographic contrast perfusion imaging would differentiate the neo-vascularization of malignancies from the avascularity of thrombi and the sparse vascularity of stromal tumors.

METHODS Sixteen patients with cardiac masses underwent power-modulation imaging after echocardiographic intravenous contrast administration. Pixel intensities in the mass and an adjacent section of myocardium were analyzed visually and by dedicated software. All masses had a pathologic diagnosis or resolved after anticoagulation. In a subset of patients, video-intensity curves of contrast replenishment in the mass and myocardium over time were generated. The post-impulse steady-state pixel intensity (A) and initial rate of contrast replenishment after impulse (β) were compared with an index of blood vessel area on pathology.

RESULTS In seven of 16 patients, contrast enhancement resulted in greater pixel intensity in the mass than in the adjacent myocardium. All of these masses were classified pathologically as malignant (n = 6) or benign and vascular (n = 1). Nine masses demonstrated decreased pixel intensity, compared with the myocardium, and were diagnosed pathologically as myxomas (n = 2) or thrombi (n = 5), or they resolved with anticoagulation (n = 2). For the subset of patients, β correlated with the vessel area index (r = 0.60).

CONCLUSIONS Echocardiographic contrast perfusion imaging aids in the differentiation of cardiac masses. Compared with the adjacent myocardium, malignant and vascular tumors hyper-enhanced, whereas stromal tumors and thrombi hypo-enhanced. (J Am Coll Cardiol 2004;43:1412–9)

Two-dimensional echocardiography is regarded as the primary diagnostic imaging technique for the evaluation of cardiac mass lesions, with a diagnostic sensitivity of 93% for transthoracic echocardiography and 97% for transesophageal echocardiography (1). However, differentiation between different types of cardiac masses, including thrombi and benign and malignant tumors, may be difficult at times. Yet, this distinction provides important diagnostic and prognostic information and guides therapeutic decision-making.

See page 1420

Microbubble contrast agents have been used with two-dimensional echocardiography to delineate the myocardium-blood interface, to define intracavitary structures, and to evaluate myocardial perfusion (2–4). The development of second-generation contrast agents and new imaging techniques, such as power modulation, have greatly improved the echocardiographic ability to assess myocardial perfusion. Qualitative and quantitative methods now exist to differentiate reliably between normal, ischemic, and infarcted myocardial tissues by their level of echocardiographic contrast perfusion (5,6).

We hypothesized that perfusion imaging could also be used to help characterize the vascularity of cardiac masses. In particular, we hypothesized that enhancement with echocardiographic contrast imaging would differentiate the neo-vascularization of a malignancy or vascular tumor from the avascularity of a thrombus and the sparse vascularity of a benign stromal tumor and that the level of enhancement would correlate with the diagnosis made by the gold standards of pathologic analysis or resolution of the mass after anticoagulant therapy.

METHODS

Patient population. Sixteen patients (12 females and 4 males; age range 19 to 84 years) with intracardiac or pericardial masses underwent perfusion imaging with echocardiographic contrast at the University of Chicago's Non-

From the Adult Noninvasive Cardiac Imaging Laboratories, Section of Cardiology; and the Department of Pathology, University of Chicago, Chicago, Illinois.

Manuscript received June 23, 2003; revised manuscript received August 26, 2003, accepted September 9, 2003.

Abbreviations and Acronyms

A = post-impulse maximal steady-state intensity level
ROI = region of interest
VAI = vessel area index

invasive Imaging Laboratory from September 1999 to January 2003. This study was approved by the Institutional Review Board of the University of Chicago Hospitals.

Echocardiographic imaging and analysis. After a slow intravenous push (0.6 to 1.0 ml) of Optison (Amersham Health, Princeton, New Jersey) or continuous intravenous infusion (infusion rate adjusted for optimal enhancement of the mass) of Definity (Bristol-Meyers Squibb, New York, New York), the masses were imaged using gray-scale power modulation (SONOS 5500, Philips Medical Systems, Andover, Massachusetts) in either real-time or a triggered mode with a low mechanical index (0.1), and the gain and compression settings were optimized for visualization of perfusion of the mass (typically within a range of 40% to 80%). The focus was set at the level of the mass. Whenever a mass demonstrated perfusion with echocardiographic contrast, an ultrasound impulse of high mechanical index (1.0 to 1.6) was transmitted for four up to 10 frames, as needed, to destroy microbubbles within the mass. This prevented the recording of "false-positive perfusion" due to a saturation artifact secondary to high gain settings. Perfusion of the mass was then confirmed by visualizing gradual contrast replenishment of the mass after the high-mechanical index impulse.

Contrast enhancement was assessed both visually, by an experienced reader familiar with contrast perfusion imaging, and using dedicated software (Qlab, Philips Medical Systems). Because absolute pixel intensity is subject to variations in contrast infusion rates and depth of masses, the perfusion in a mass is meaningfully assessed only in relation to the perfusion in the adjacent myocardium. A discrete region of interest (ROI) was drawn both within the central part of each mass and within a section of adjacent ventricular myocardium. Care was taken not to draw ROIs in areas of the myocardium that demonstrated a lack of perfusion. The ROI locations were adjusted to correct for translational motion. The mean pixel intensities within the ROIs were measured for each frame in at least two cardiac cycles. The difference between the mean pixel intensity of the mass and that of the adjacent myocardium was computed.

To assess the interobserver variability of the visual interpretation of mass perfusion, three blinded expert readers were asked to assess the level of contrast within the mass. Their responses were compared with those of the original reader, with a weighted kappa statistic.

In addition, three less experienced readers with no training in contrast perfusion imaging were shown non-contrast images of each mass and diagnosed the mass as malignancy/vascular tumor, stromal tumor, or thrombus. They were then shown contrast perfusion images of each mass and again made a diagnosis. These answers were compared against the gold standard of pathologic diagnosis, and a Wilcoxon matched-pairs signed-rank test was used to assess the incremental benefit of contrast in improving diagnostic accuracy.

Table 1. Contrast Perfusion and Pathologic Diagnosis of Cardiac Masses

Patient Number	Location of Mass	Mean Pixel Intensity (dB) of Mass	Mean Pixel Intensity (dB) of Myocardium	Pathology
1	Pulmonary artery, extension from mediastinal mass encasing great vessels	11	8.2	Anaplastic large-cell lymphoma
2	RA, originating in SVC	15	11	Follicular thyroid carcinoma
3	RV apex	3.7	1	Malignant peripheral nerve sheath tumor
4	LV apex	25	19	Hemangioma
5	Pleura and pericardium near apical-lateral LV	15	6.5	Lung adenocarcinoma
6	Apical pericardium	30	16	Poorly differentiated adenocarcinoma, unknown primary
7	Apical pericardium	18	15	Well-differentiated adenocarcinoma of the lung
8	LA, attached to fossa ovalis	10	16	Myxoma
9	LA side of interatrial septum	7.7	7.8	Myxoma
10	RA free wall near IVC	5.5	6.5	Resolution demonstrated on echocardiogram after 2 months of anticoagulation
11	RA free wall	4.8	8.1	Thrombus (resected for anticoagulation contraindication)
12	LV apex, pedunculated	0.1	6.5	Thrombus (resected for anticoagulation contraindication)
13	LV apex	0.2	17	Thrombus on autopsy
14	LV apex	7.1	29	Resolution demonstrated on follow-up echocardiogram
15	LV apex	4.1	13	Thrombus (resected during coronary artery bypass)
16	LV apex	20	29	Mural thrombus on autopsy

IVC = inferior vena cava; LA = left atrial; LV = left ventricle/ventricular; RA = right atrial; SVC = superior vena cava.

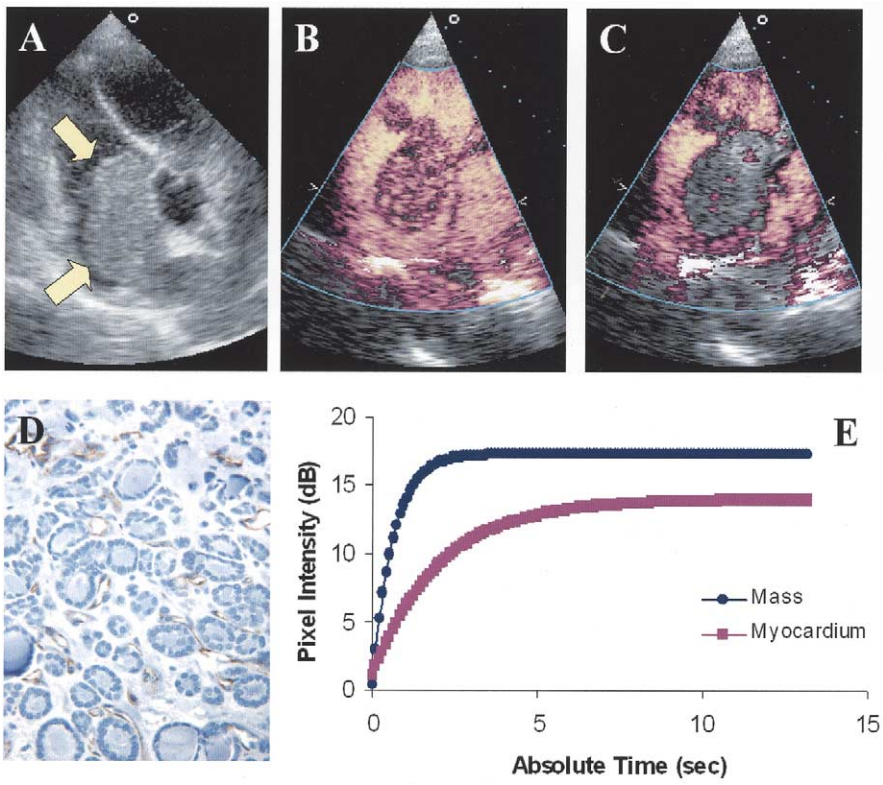

Figure 1. **(A)** A mass filling the right atrium (apical five-chamber view). **(B)** The mass hyper-enhanced with echocardiographic contrast, compared with the adjacent myocardium. **(C)** There was no enhancement of the mass or the adjacent myocardium after a high-mechanical index impulse destroyed contrast bubbles, ruling out "false-positive perfusion" of the mass. **(D)** The biopsy specimen diagnosis was follicular thyroid carcinoma. The blood vessels are stained with CD31 antibody. **(E)** Perfusion curves of video intensity over time demonstrated greater values for A and β for the mass than for the adjacent myocardium.

Pathologic correlation. The echocardiographic findings were then compared with the pathologic diagnosis for each mass (n = 14) or the results of follow-up imaging studies demonstrating resolution of the mass after anticoagulant therapy (n = 2).

Quantitative analysis of perfusion. In a subset of seven patients, further quantitative analysis was performed. Video loops were triggered to acquire end-systolic frames. The mean pixel intensity after a high mechanical impulse was then simultaneously calculated frame by frame for both the mass and a section of adjacent myocardium and fitted with the following exponential function of time (7):

$$y = A \cdot (1 - e^{-\beta \cdot t})$$

where A reflects the post-impulse maximal steady-state intensity level (a surrogate measure for vascular volume) and β represents the initial rate of contrast replenishment after the high-mechanical index impulse (reflecting the velocity of blood flow) (8). The A and β values for each mass were subtracted from the A and β values for the section of adjacent myocardium to account for differences in contrast infusion rate and depth of mass.

The biopsy specimens for these seven masses were stained with a variety of monoclonal antibodies directed against antigens found in the endothelium, including factors VIII, CD31, and CD34. The slide that demonstrated the clearest staining of vascular structures with the least amount of background staining was analyzed to determine a vessel area index (VAI) as follows. For each biopsy specimen, the power of magnification (either 10× or 40×) that demonstrated the best image of the vessels for accurate cross-sectional area measurement was chosen. In specimens for which the 10× power was used, all vessels were measured in a total of 10 fields to obtain an accurate representation of the entire biopsy specimen. The 40× power was used in the case of smaller sized vessels, and a total of 25 fields were measured. Using a dedicated software program (Leica AS LMD, version 3.1, Leica Microsystems, Bannockburn, Illinois), lines were drawn to outline the lumen of vessels in each field, and the cross-sectional area of each vessel was computed in μm^2. To compare the sizes of the vessels between specimens, the diameter of greatest dimension was computed in μm using the same software program for 50 random vessels in each specimen. The average vessel diameter and range for each specimen were calculated. For each biopsy specimen, the total cross-sectional area of all vessels measured was calculated and divided by the total area covered in all the fields viewed to obtain the VAI.

RESULTS

Echocardiographic imaging and analysis. Seven masses demonstrated enhancement with echocardiographic con-

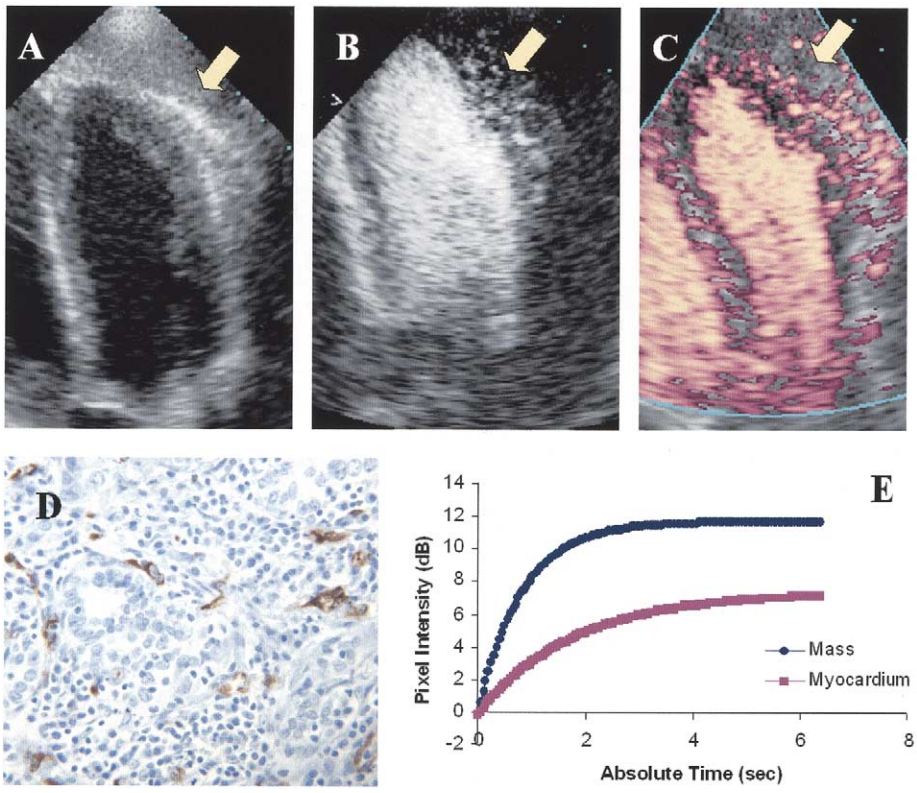

Figure 2. **(A)** A mass adjacent to the lateral wall of the left ventricle (apical four-chamber view). **(B)** There was hyperenhancement of the mass, relative to the adjacent myocardium. **(C)** There was no enhancement of the mass or the adjacent myocardium after a high-mechanical index impulse destroyed microbubbles. **(D)** A biopsy specimen stained with factor VIII antibody demonstrated extensive vascularity in a poorly differentiated adenocarcinoma. **(E)** Perfusion curves of video intensity over time demonstrated greater values for A and β for the mass than for the adjacent myocardium.

trast, both visually and on quantitative analysis. In each case, the mean pixel intensity over the cardiac cycle of the mass was higher than that of the adjacent myocardium. Two masses demonstrated partial and/or incomplete enhancement with contrast upon visual inspection; the mean pixel intensity was lower than that of the myocardium. Seven of the masses failed to enhance upon visual inspection and had a lower mean pixel intensity than that of the myocardium (Table 1). The weighted kappa values for interobserver variability on visual assessment of perfusion ranged from 0.75 to 0.84.

Contrast perfusion imaging improved the less experienced readers' accuracy in differentiating between malignancy/vascular tumor, stromal tumor, and thrombus. The total number of correct diagnoses for all three readers increased from 34 to 41 (of 48 possible) with the addition of contrast perfusion imaging. The Wilcoxon matched-pairs signed-rank test yielded a two-tailed p value of 0.06.

Pathologic correlation. The seven patients who had cardiac masses demonstrating greater enhancement than the adjacent myocardium were diagnosed with malignant or highly vascular tumors by pathologic analysis. The two masses that enhanced partially on visual inspection were confirmed pathologically to be myxomas (n = 2). Of the seven masses that failed to enhance, five were pathologically confirmed to be thrombi at the time of cardiac surgery, whereas two resolved on anticoagulation therapy (Table 1).

Quantitative analysis of perfusion. Video-intensity curves for contrast perfusion, echocardiographic images, and pathologic specimens for the subset of seven masses are shown in Figures 1 through 5. Table 2 details pathologic diagnoses, vessel size range, pathologic VAI, and differences between the A and β values of mass and myocardium for the subset. Relative to the adjacent myocardium, malignant (n = 4) and vascular benign (n = 1) tumors demonstrated a more rapid increase in perfusion and higher steady-state perfusion: the mean difference in β between each mass and section of adjacent myocardium (mean $\Delta\beta_{\text{mass}-\text{myocardium}}$) was 1.3/s (range −0.1 to 2.7), and the mean difference in A between each mass and section of adjacent myocardium (mean $\Delta A_{\text{mass}-\text{myocardium}}$) was 6.8 dB (range 4.0 to 13). The thrombi did not perfuse, as illustrated by the flat line in Figure 3. The correlation coefficients for $\Delta A_{\text{mass}-\text{myocardium}}$ and VAI and for $\Delta\beta_{\text{mass}-\text{myocardium}}$ and VAI were 0.36 and 0.60, respectively.

DISCUSSION

Using contrast echocardiography, our study found qualitative and quantitative differences in the gray scale between the levels of perfusion in various types of cardiac masses and sections of adjacent myocardium. These differences were detected using power modulation and dedicated video-intensity detection software. Malignant or highly vascular

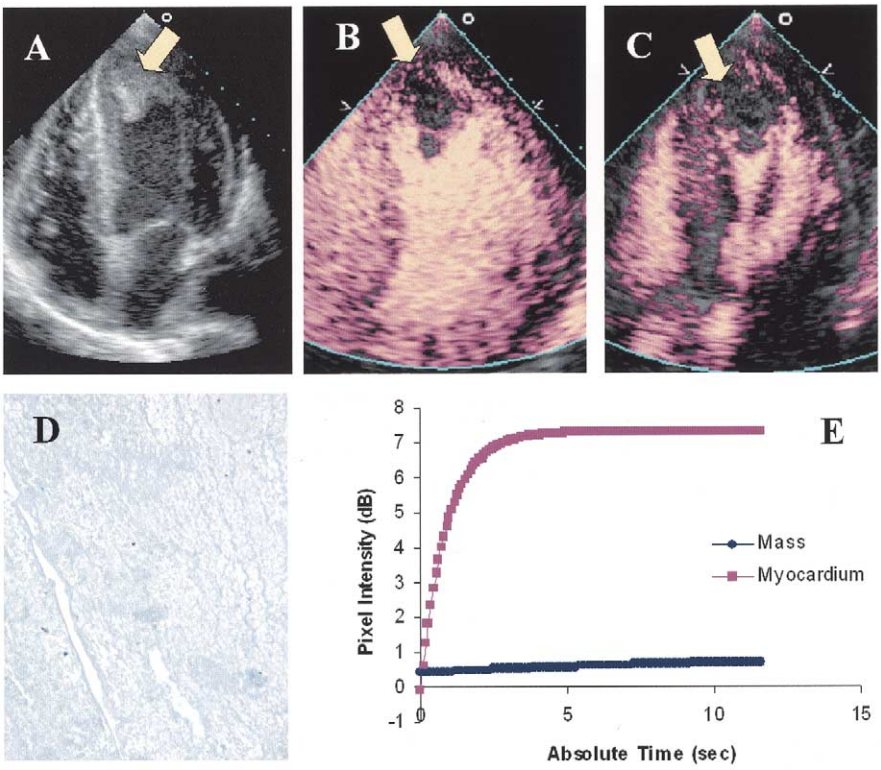

Figure 3. (A) A left ventricular apical mass (apical four-chamber view). **(B)** The mass showed no enhancement with contrast, whereas the adjacent myocardium demonstrated enhancement. **(C)** There was no enhancement of the mass or adjacent myocardium after a high-mechanical index impulse destroyed the contrast agent. **(D)** The surgical specimen demonstrated no staining with CD34 antibody and minimal cellularity, consistent with thrombus. **(E)** Perfusion curves of video intensity over time demonstrated no increase in video intensity in the mass from baseline, whereas video intensity increased within the myocardium.

tumors demonstrated greater enhancement than the adjacent myocardium. Myxomas demonstrated partial perfusion on visual inspection and quantitatively less perfusion than the myocardium. The thrombi in this study demonstrated no perfusion. With the aid of contrast, perfusion imaging identified three pericardial malignancies—an area that has traditionally been a challenge to evaluate with echocardiography. The addition of contrast perfusion to standard imaging demonstrated a trend toward improving the ability of readers without training in this technique to diagnose cardiac masses, although the number of data points likely precluded detection of a statistically significant improvement. In a subset of seven masses, the difference in the rate of increase in pixel intensity after a high mechanical impulse between the mass and adjacent myocardium ($\Delta\beta_{\text{mass}-\text{myocardium}}$) demonstrated a better correlation with VAI in the pathologic specimens, as compared with the difference in the maximum steady-state pixel intensity between the mass and myocardium ($\Delta A_{\text{mass}-\text{myocardium}}$).

The etiology of cardiac masses presents a differential diagnosis with important prognostic and therapeutic implications. Benign tumors generally portend a good prognosis. Although malignant primary cardiac tumors, if discovered early, are potentially curable with surgical resection (9), studies have consistently found a very poor prognosis and low overall rates of respectability (10–12). Thrombi may present with catastrophic embolization and warrant surgical removal in some cases, but they often resolve with noninvasive treatment (13). Although multiple echocardiographic criteria are used to define cardiac masses (14–18), there are frequent reports in the medical literature of diagnostic errors (19–21). Misclassifications can lead to unfortunate outcomes from an unnecessary surgical procedure or inappropriate exposure to the risks of anticoagulation.

Myocardial tissue is highly vascular (capillary density on the order of 2,500 to 3,000/mm^3) (22), but most malignancies have abnormal neo-vascularization that supplies rapidly growing tumor cells, often in the form of highly concentrated, dilated vessels, as depicted in Figures 1, 2, and 5 (23). The total blood-carrying capacity of these vessels is likely to be in excess of that of the adjacent myocardium. Stromal tumors, such as myxomas, have a poor blood supply. Thrombi are generally avascular (Fig. 3). Sensitive measures of tissue perfusion should therefore be able to detect differences between neo-vascularized malignant or highly vascular cardiac tumors, poorly vascularized stromal tumors, avascular thrombi, and normal myocardium.

Contrast echocardiography to characterize myocardial perfusion has benefited in recent years from the development of new microbubble agents that can be administered intravenously at a constant rate to achieve a steady-state concentration. Application of a high-mechanical index impulse leads to increased microbubble destruction; the rate of

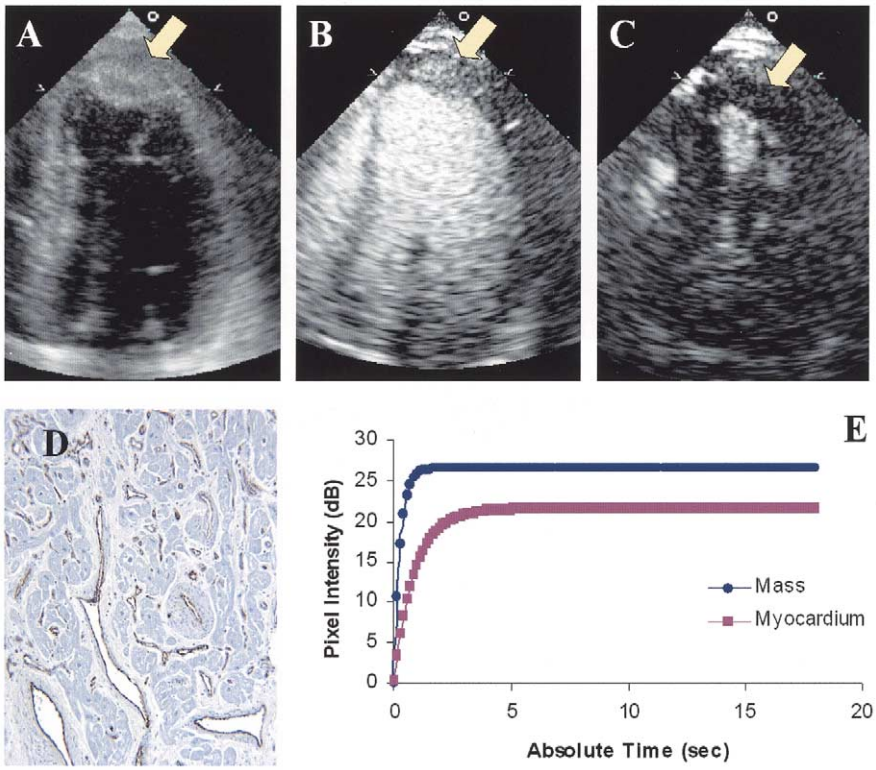

Figure 4. **(A)** A left ventricular apical mass (apical four-chamber view). **(B)** The mass hyper-enhanced with contrast, relative to the adjacent myocardium. **(C)** There was no enhancement of the mass or adjacent myocardium after a high-mechanical index impulse destroyed the contrast agent. **(D)** The surgical specimen was diagnosed as a hemangioma with abundant, dilated, thick-walled vessels, demonstrated by staining with factor VIII antibody. **(E)** Perfusion curves of video intensity over time demonstrated greater values for A and β for the mass than for the adjacent myocardium.

replenishment (β) and maximum steady-state concentration *(A)* of microbubbles in tissue after the impulse can be measured as video intensity, reflecting the degree of blood flow (24,25). The off-line use of a computer program to detect and quantify replenishment after microbubble destruction within a cardiac structure has been applied to assessment of wall motion (26) and myocardial perfusion (27,28). The application of such a program to evaluate perfusion within a cardiac mass versus an adjacent section of myocardium is, as far as we know, unique to this study.

Microbubble contrast and pulse-inversion imaging of large vessels has been used to differentiate benign from malignant tumors in the liver (29,30), but power-modulation imaging allows more sensitive detection of smaller vessels and a potentially improved correlation with pathologic blood vessel assessments than has previously been demonstrated (31). In our subset of seven patients, we used power-modulation contrast imaging to characterize the relationships between blood vessel volume, rate of blood flow in the mass, and a pathologic measure of vessel area by comparing the differences in A and β between the mass and adjacent myocardium with VAI. $\Delta\beta_{\mathrm{mass-myocardium}}$ correlated reasonably well with VAI, probably because the dilated neovessels of the malignant and highly vascular tumors in the subset filled more quickly with contrast agent than did the normal vessels of the adjacent myocardium. $\Delta A_{\mathrm{mass-myocardium}}$ did not correlate well with VAI, perhaps because the relatively small portion of a mass that is analyzed to determine VAI may not reflect the level of perfusion detected by contrast perfusion imaging. Conversely, some of the specimens contained vessels with very small lumens, and perhaps the resolution of the pixel-intensity detection program was unable to detect the contribution of these small vessels to the maximum pixel intensity. Furthermore, as Ellegala et al. (32) have demonstrated in contrast perfusion imaging of malignant gliomas in rat brains, detection of the volume and velocity of blood flow in the tumor relative to the adjacent tissue may depend on size of the tumor.

By differentiating malignant/highly vascular tumors from benign tumors and thrombi, echocardiographic contrast perfusion imaging may aid in the early identification and appropriate treatment of cardiac masses. Primary cardiac tumors are rare, with an estimated incidence of 0.0017% to 0.28% (33). Thrombi and metastases are far more common and constitute the main elements of the differential diagnosis, unless located in the atria (suggesting myxoma) (34). Hyperenhancement, signaling probable malignancy, in a cardiac tumor may facilitate early recognition and resection, or may steer treatment planning toward palliation for certain patients who wish to avoid invasive and probably futile interventions. A complete lack of enhancement, signaling thrombus, would be an indication for anticoagulation with a follow-up imaging study to evaluate resolution and

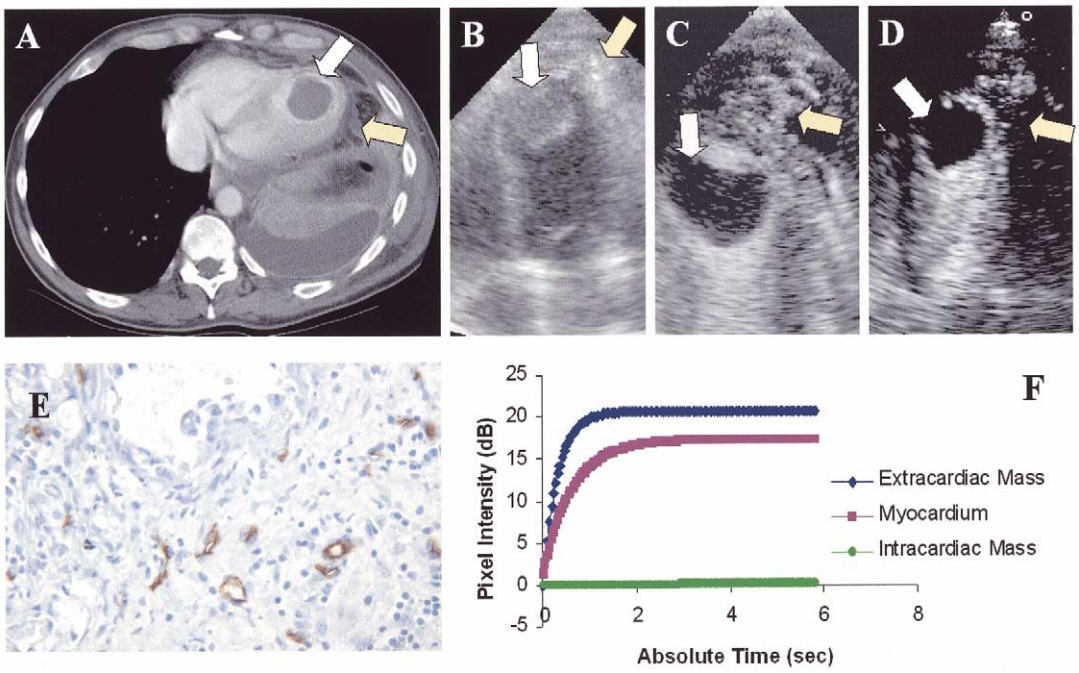

Figure 5. **(A)** A computed tomographic scan of the chest with contrast demonstrating an intracardiac mass **(white arrow)** and a hypodense area in the lung parenchyma **(yellow arrow)**. **(B)** Apical four-chamber view of the left ventricular (LV) apical mass **(white arrow)** and the mass extrinsic to the LV apex **(yellow arrow)**. **(C)** The LV apical mass failed to enhance with contrast, whereas the extrinsic mass hyper-enhanced, relative to the myocardium, and demonstrated large vascular channels **(yellow arrow)**. **(D)** There was no enhancement of the masses or adjacent myocardium after a high-mechanical index impulse destroyed the microbubbles. **(E)** The biopsy specimen of the extrinsic mass showed a well-differentiated adenocarcinoma with multiple vascular channels stained with CD34 antibody. Lacking pathologic correlation, the intracardiac mass was not included in the comparison of contrast perfusion with VAI and does not appear in Table 2. **(F)** Perfusion curves of video intensity over time demonstrated greater values for A and β for the mass than for the adjacent myocardium and no increase in intensity from baseline for the intracardiac mass. The intracardiac mass was presumed to be a thrombus.

could prevent unnecessary cardiac surgery. A further application is the detection and evaluation of malignant or highly vascular tumors or metastases within the myocardium that do not protrude into cardiac chamber cavities. Objective hyperenhancement of one area of the myocardium may raise the suspicion for intramyocardial tumor infiltration.

Study limitations. Although myxomas appeared to demonstrate partial enhancement on visual inspection, thrombi and myxomas could not be differentiated objectively on the basis of average pixel intensity in the mass relative to myocardium. An assessment of $\Delta A_{\text{mass}-\text{myocardium}}$ and $\Delta\beta_{\text{mass}-\text{myocardium}}$ was performed in only seven patients. Because of the differences in depth of the masses and the differing amounts of perfusion between different patients, we were unable to compare pixel intensity between the different types of masses and instead had to compare the differences in perfusion relative to the adjacent myocardium. Not all of our pathologic specimens contained myocardial tissue, and we were unable to evaluate any possible effect that differences in myocardial VAI between patients may have had on ΔA and $\Delta\beta$.

Conclusions. We found that quantification of echocardiographic perfusion imaging of cardiac masses with gray-scale power modulation facilitates the differential diagnosis of cardiac masses. Malignant and highly vascular tumors became visually hyper-enhanced and demonstrated quantitatively more perfusion than the adjacent myocardium. Stromal tumors demonstrated partial enhancement and less

Table 2. Subset of Masses With Quantitative Echocardiographic Perfusion

Patient Number	Pathologic Diagnosis	Vessel Diameter Average in μm (range)	VAI	$\Delta A_{\text{mass}-\text{myocardium}}$	$\Delta\beta_{\text{mass}-\text{myocardium}}$
2	Follicular thyroid carcinoma in RA (Fig. 1)	10 (2.0–68)	0.024	4	1.1
6	Poorly differentiated adenocarcinoma in apical pericardium (Fig. 2)	17 (2.0–159)	0.013	5.9	0.5
12	Thrombus in LV apex (Fig. 3)	5.2 (2.0–36)	0.0010	−6.3	−1.1
4	Hemangioma in LV apex (Fig. 4)	63 (2.0–608)	0.040	5.3	2.5
7	Adenocarcinoma of lung in apical pericardium (Fig. 5)	11 (2.0–56)	0.017	13	2.7
11	Thrombus on RA free wall	2.6 (1.0–5.0)	0.000017	−4.7	−0.51
1	Lymphoma in pulmonary artery	63 (14–454)	0.020	5.9	−0.12

A = maximum steady-state pixel intensity (dB); β = rate of increase in pixel intensity (1/s); VAI = vessel area index: total cross-sectional area of blood vessels (μm^2)/total area of high-power fields (μm^2). Other abbreviations as in Table 1.

perfusion than the adjacent myocardium. Thrombi failed to enhance. With the application of contrast perfusion imaging, there was a trend toward improving the ability of readers with no training in this technique to differentiate between these types of tumors. In a subset of seven patients, the rate of increase in pixel intensity over time correlated with the cross-sectional vessel area of the pathologic specimen. This technique could be easily applied in echocardiographic laboratories with contrast perfusion imaging capabilities.

Reprint requests and correspondence: Dr. Roberto M. Lang, University of Chicago Adult Noninvasive Imaging Laboratory, 5841 South Maryland Avenue, MC 5084, Chicago, Illinois 60637. E-mail: rlang@medicine.bsd.uchicago.edu.

REFERENCES

1. Meng Q, Lai H, Lima J, Tong W, Qian Y, Lai S. Echocardiographic and pathologic characteristics of primary cardiac tumors: a study of 149 cases. Int J Cardiol 2002;84:69–75.
2. Sieswerda GT, Kamp O, Visser CA. Myocardial contrast echocardiography: clinical benefit and practical issues. Echocardiography 2000; 17:S25–36.
3. Lindner JR. Assessment of myocardial viability with myocardial contrast echocardiography. Echocardiography 2002;19:417–25.
4. Mengozzi G, Rossini R, Palagi C, et al. Usefulness of intravenous myocardial contrast echocardiography in the early left ventricular remodeling in acute myocardial infarction. Am J Cardiol 2002;90: 713–9.
5. Wei K, Crouse L, Weiss J, et al. Comparison of usefulness of dipyridamole stress myocardial contrast echocardiography to technetium-99m sestamibi single-photon emission computed tomography for detection of coronary artery disease (PB127 multicenter phase 2 trial results). Am J Cardiol 2003;91:1293–8.
6. Van Camp G, Ay T, Pasquet A, et al. Quantification of myocardial blood flow and assessment of its transmural distribution with real-time power modulation myocardial contrast echocardiography. J Am Soc Echocardiogr 2003;16:263–70.
7. Wiencek JG, Feinstein SB, Walker R, Aronson S. Pitfalls in quantitative contrast echocardiography: the steps to quantitation of perfusion. J Am Soc Echocardiogr 1993;6:395–416.
8. Wei K, Jayaweera AR, Firoozan S, Linka A, Skyba DM, Kaul S. Quantification of myocardial blood flow with ultrasound-induced destruction of microbubbles administered as a constant venous infusion. Circulation 1998;97:473–83.
9. Goldman JH, Foster E. Transesophageal echocardiographic (TEE) evaluation of intracardiac and pericardial masses. Cardiol Clin 2000; 18:849–60.
10. Perchinsky MJ, Lichtenstein SV, Tyers GF. Primary cardiac tumors: forty years' experience with 71 patients. Cancer 1997;79:1809–15.
11. Grande AM, Ragni T, Vigano M. Primary cardiac tumors: a clinical experience of 12 years. Tex Heart Inst J 1993;20:223–30.
12. Molina JE, Edwards JE, Ward HB. Primary cardiac tumors: experience at the University of Minnesota. Thorac Cardiovasc Surg 1990;38 Suppl 2:183–91.
13. Greaves SC, Zhi G, Lee RT, et al. Incidence and natural history of left ventricular thrombus following anterior wall acute myocardial infarction. Am J Cardiol 1997;80:442–8.
14. Lynch M, Clements SD, Shanewise JS, Chen CC, Martin RP. Right-sided cardiac tumors detected by transesophageal echocardiography and its usefulness in differentiating the benign from the malignant ones. Am J Cardiol 1997;79:781–4.
15. Gopal AS, Stathopoulos JA, Arora N, Banerjee S, Messineo F. Differential diagnosis of intracavitary tumors obstructing the right ventricular outflow tract. J Am Soc Echocardiogr 2001;14:937–40.
16. Lepper W, Shivalkar B, Rinkevich D, Belcik T, Wei K. Assessment of the vascularity of a left ventricular mass using myocardial contrast echocardiography. J Am Soc Echocardiogr 2002;15:1419–22.
17. Mottram PM, Gelman JS. Mitral valve thrombus mimicking a primary tumor in the antiphospholipid syndrome. J Am Soc Echocardiogr 2002;15:746–8.
18. Hasegawa T, Nakagawa S, Chino M, Kunihiro T, Ui S, Kimura M. Primary cardiac sarcoma mimicking benign myxoma: a case report. J Cardiol 2002;39:321–5.
19. Alam M. Pitfalls in the echocardiographic diagnosis of intracardiac and extracardiac masses. Echocardiography 1993;10:181–91.
20. Menegus MA, Greenberg MA, Spindola-Franco H, Fayemi A. Magnetic resonance imaging of suspected atrial tumors. Am Heart J 1992;123:1260–8.
21. Robinson NM, Desai J, Monaghan MJ. Atrial and pulmonary mass: intracardiac thrombus mimicking myxoma on multiplane transesophageal echocardiography. J Am Soc Echocardiogr 1997;10:93–6.
22. Le DE, Bin JP, Coggins MP, Wei K, Lindner JR, Kaul S. Relation between myocardial oxygen consumption and myocardial blood volume: a study using myocardial contrast echocardiography. J Am Soc Echocardiogr 2002;15:857–63.
23. Fidler IJ. Critical factors in the biology of human cancer metastasis. Am Surg 1995;61:1065–6.
24. Spencer KT, Grayburn PA, Mor-Avi V, et al. Myocardial contrast echocardiography with power Doppler imaging. Am J Cardiol 2000; 86:479–81.
25. Kaul S. Myocardial contrast echocardiography: 15 years of research and development. Circulation 1997;96:3745–60.
26. Caiani EG, Lang RM, DeCara J, et al. Objective assessment of left ventricular wall motion from contrast-enhanced power modulation images. J Am Soc Echocardiogr 2002;15:118–28.
27. Lindner JR, Villanueva FS, Dent JM, Wei K, Sklenar J, Kaul S. Assessment of resting perfusion with myocardial contrast echocardiography: theoretical and practical considerations. Am Heart J 2000; 139:231–40.
28. Masugata H, Peters B, Lafitte S, Strachan GM, Ohmori K, DeMaria AN. Quantitative assessment of myocardial perfusion during graded coronary stenosis by real-time myocardial contrast echo refilling curves. J Am Coll Cardiol 2001;37:262–9.
29. Wilson SR, Burns PN. Liver mass evaluation with ultrasound: the impact of microbubble contrast agents and pulse inversion imaging. Semin Liver Dis 2001;21:147–59.
30. Harvey CJ, Blomley MJ, Eckersley RJ, et al. Hepatic malignancies: improved detection with pulse-inversion US in late phase of enhancement with SH U 508A—early experience. Radiology 2000;216:903–8.
31. Yang WT, Tse GM, Lam PK, Metreweli C, Chang J. Correlation between color power Doppler sonographic measurement of breast tumor vasculature and immunohistochemical analysis of microvessel density for the quantitation of angiogenesis. J Ultrasound Med 2002;21:1227–35.
32. Ellegala DB, Leong-Poi H, Carpenter JE, et al. Imaging tumor angiogenesis with contrast ultrasound and microbubbles targeted to alpha(v)beta3. Circulation 2003;108:336–41.
33. Dhillon G, Rodriguez-Cruz E, Kathawala M, Alqassem N. Primary cardiac myofibroblastic sarcoma: case report and review of diagnosis and treatment of cardiac tumors. Bol Asoc Med P R 1998;90:130–3.
34. Gibbs P, Cebon JS, Calafiore P, Robinson WA. Cardiac metastases from malignant melanoma. Cancer 1999;85:78–84.